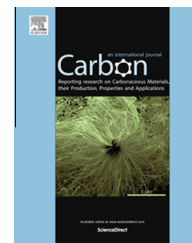


Available at www.sciencedirect.com

ScienceDirect

journal homepage: www.elsevier.com/locate/carbon

Nano-graphite cold cathodes for electric solar wind sail

Victor I. Kleshch ^a, Elena A. Smolnikova ^a, Anton S. Orekhov ^b, Taneli Kalvas ^c,
Olli Tarvainen ^c, Janne Kauppinen ^c, Antti Nuottajärvi ^{c,d}, Hannu Koivisto ^c,
Pekka Janhunen ^e, Alexander N. Obratsov ^{a,f,*}

^a Department of Physics, M.V. Lomonosov Moscow State University, Moscow 119991, Russia

^b A.V. Shubnikov Institute of Crystallography, RAS, Moscow 119333, Russia

^c Department of Physics, University of Jyväskylä, Jyväskylä 40014, Finland

^d Department of Chemistry and Bioengineering, Tampere University of Technology, Tampere 33720, Finland

^e Finnish Meteorological Institute, Helsinki 00560, Finland

^f Department of Physics and Mathematics, University of Eastern Finland, Joensuu 80101, Finland

ARTICLE INFO

Article history:

Received 4 June 2014

Accepted 12 September 2014

Available online xxxx

ABSTRACT

The nanographite (NG) films consisting of tiny graphite crystallites (nanowalls) are produced by carbon condensation from methane–hydrogen gas mixture activated by a direct current discharge. High aspect ratio and structural features of the NG crystallites provides efficient field electron emission (FE). Applicability and performance of the NG films in an electron gun (E-gun) of a solar wind thruster system with an electric sail (E-sail) is tested. The long-term tests are demonstrated suitability of E-gun assembly with the NG cathodes for the real space missions. The results of the tests are analyzed and physical mechanisms of the cathode aging and practical methods for improvement performance of the E-gun are proposed.

© 2014 Elsevier Ltd. All rights reserved.

1. Introduction

The electric sail (E-sail) is a new method of propelling a spacecraft by using solar wind as a thrust source [1,2]. The E-sail spacecraft consists of long conductive tethers which are centrifugally stretched by spacecraft spin. In order to generate an electrostatic field, that deflects solar wind ions, the tethers must be positively charged at high voltage. The scattered solar wind ions lose part of the flow-aligned component of their momentum which gets transmitted to the tethers and to the spacecraft that experiences corresponding propulsive acceleration. The positive voltage of the tethers can be obtained by using an electron gun (E-gun) that removes neg-

atively charged electrons from the system by smoothing them away into the surrounding solar wind plasma. Field emission (FE) cold cathodes are especially attractive for this application, taking into account necessity to provide efficient electron emission with minimal energy consumption due to energy deficiency at the spacecraft, especially in the CubeSat-scale E-sail test missions [3,4]. In this work we analyze applicability of the nano-graphite (NG) films as cold cathodes for the E-sail system. The tests described below were made for the laboratory prototypes of the E-gun (see Fig. 1). In our next publications, we will report results of further tests that are performed at present time in a space mission of EstCube-1 [5].

* Corresponding author at: Department of Physics, M.V. Lomonosov Moscow State University, Moscow 119991, Russia.

E-mail address: obraz@polly.phys.msu.ru (A.N. Obratsov).

<http://dx.doi.org/10.1016/j.carbon.2014.09.038>

0008-6223/© 2014 Elsevier Ltd. All rights reserved.

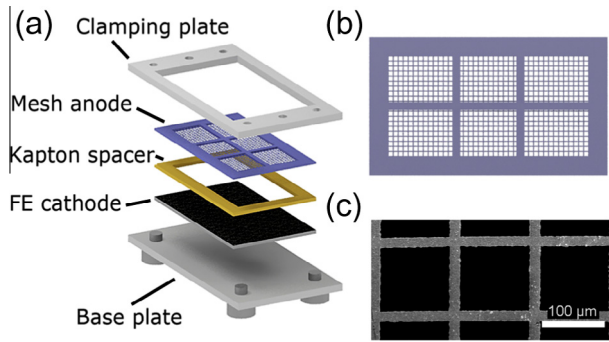


Fig. 1 – (a) Scheme of the electron gun with a field emission cold NG cathode; FE cathode (NG film on Ni substrate) is separated from a copper mesh anode by a kapton spacer of 50–100 μm thickness. (b) Scheme of the mesh anode made from $\text{Si}_3\text{N}_4\text{-Si-Si}_3\text{N}_4$ wafer by semiconductor micromachining techniques with 1 μm thick Cu film evaporated on it. (c) Scanning electron microscopy image of the copper mesh cells. (A color version of this figure can be viewed online.)

2. Experimental

In the laboratory prototype of the E-gun (Fig. 1a) the NG cathodes were separated from a copper mesh anode by a kapton insulating spacer with thickness of 50–100 μm . The cathode, spacer and mesh were fixed with insulating screws between aluminum base plate and clamping plate. The anode mesh (Fig. 1b) was made from 300 μm thick $\text{Si}_3\text{N}_4\text{-Si-Si}_3\text{N}_4$ wafer by chemically wet etching six rectangular areas, where 100 \times 100 μm mesh with 1 μm thick and 6 μm wide Si_3N_4 bars was processed by reactive ion etching (Fig. 1c). The separation of the mesh into 6 areas was done to improve mechanical rigidity. The mesh was made electrically conductive by coating it with a 1 μm thick copper layer.

The NG cathodes were produced by carbon condensation from methane–hydrogen gas mixture activated by direct current discharge on Ni substrates of 22.4 \times 13.0 mm^2 size and 0.5 mm thickness using chemical vapor deposition (CVD) techniques described elsewhere [6]. One of the most essential properties of the NG CVD films is their composition of tiny graphite flakes. Each of the flakes is composed of a few graphene layers standing perpendicular to substrate surface. High aspect ratio of the conductive flakes and strong interatomic bonding, which are specific for graphite, provide excellent field electron emission characteristics of the NG cathodes. Applicability this type of cold cathodes for vacuum electronic devices has been demonstrated previously [7,8].

The aim of this work was to test the E-guns with the NG cathodes at conditions and regimes close to that expected in the real space missions. In particular, estimations show that in working regime E-gun should operate at total current of 2–5 mA and voltage of about 200 V [2,9]. These parameters were used for the tests in vacuum of 10^{-6} – 10^{-7} mbar. Before and after these tests each of the NG cathodes was analyzed to determine its FE characteristics, structure and morphological properties with use of Raman spectroscopy and scanning

electron microscopy (SEM). The Raman measurements were performed with Jobin Yvon U-1000 spectrometer using 514.5 nm Ar-ion laser excitation. The SEM inspections were performed using a Zeiss Leo 1550 instrument. The FE characteristics were measured in vacuum of about 10^{-6} mbar to establish current vs. voltage dependencies and emission site distribution with use of a phosphor coated transparent anode screen [7,8]. During the measurements, performed in vacuum of about 10^{-6} – 10^{-7} mbar, the distance between tested sample (cathode) and anode was established of about 300 μm . The emission current dependencies were measured with Keithley picoammeter (model 6485) with use of ramping voltage applied between the cathode and anode. The images, produced on transparent anode screen, covered by phosphor material, by the FE electrons and corresponding to emission site distributions, were captured with a digital camera.

3. Results and discussion

A typical dependence of FE current density, J , on electric field strength, E , measured together with corresponding FE pattern (image produced by electrons emitted from the cathode on the phosphor coated transparent anode screen) for as-grown NG film is shown in Fig. 2. The measurements were performed by applying ramping voltage between the cathode and anode separated by the vacuum gap of 300 μm . The as-grown NG cathodes demonstrated threshold field value of about 1 $\text{V}/\mu\text{m}$ at current density of 0.01 mA/cm^2 and uniform FE patterns with density of emission sites up to 10^6cm^{-2} . J - E characteristic in Fowler–Nordheim coordinates (inset in Fig. 2a) followed a linear dependence, which is typical for field emitters with metallic type of conductivity. These results are in agreement with previous investigations of the NG films [7,8].

An example of a long-term E-gun test is shown in Fig. 3. In the test constant voltage of 350 V was applied between the cathode and mesh anode and FE current of the cathode was measured. The gradual current reduction was detected during

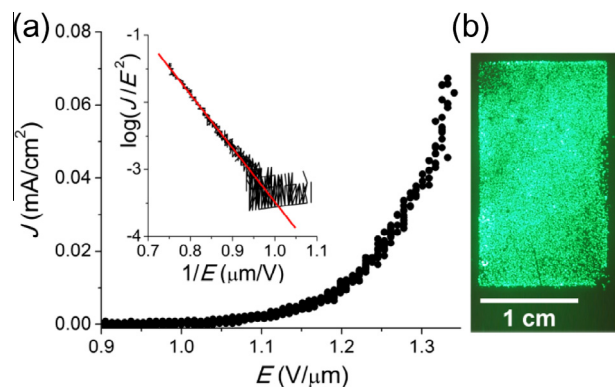


Fig. 2 – (a) An example of the dependence of FE current density J on electrical field strength E of the as-grown NG cathode. Inset shows J - E dependence in Fowler–Nordheim coordinates and its linear fit. (b) Typical FE pattern demonstrating homogeneous distribution of emission sites for the NG cathode. (A color version of this figure can be viewed online.)

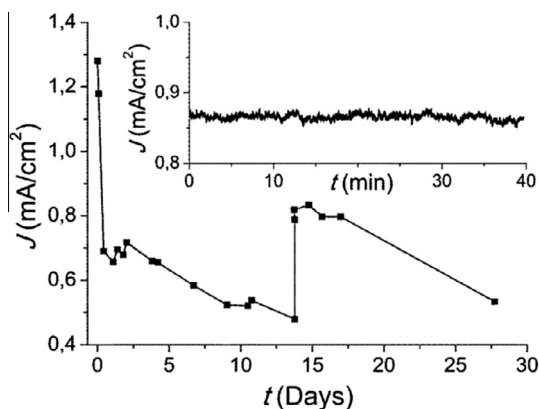


Fig. 3 – Dependence of FE current density J on time t during long-term test of the E-gun with initial voltage of 350 V and final voltage of 380 V after adjustment at the day 14 of the test. Inset shows typical dependence of FE current density on time at minute timescale obtained at field intensity of 3.4 V/ μ m at voltage applied between NG cathode and anode mesh of 380 V.

the test. The voltage adjustment to 380 V was made in order to raise current density level to the value, corresponding E-gun working regime, close to 1 mA/cm² (Fig. 3).

It was found in the tests that FE current decreased on approximately 50% during first 10 h after switch on of the E-gun. Approximation of this first current drop with exponential dependence $I \sim e^{-t/T}$ gave characteristic time T_1 of about 20 h. Further, the current decrease rate was much slower with characteristic time T_2 typically in the range of 500–1000 h. Therefore, the ratio of T_2/T_1 was in the range of 25–50. Similar behavior of FE current on time, which was characterized by two time constants, was observed previously for NG cathodes measured at laboratory conditions, where the value of T_2/T_1 ratio was in the range of 10–50 [10], which is in a good agreement with current study. According to findings of Ref. [10] the first fast degradation process is connected with cathode material sputtering due to bombardment of NG film by the ions of residual gases. The second slow degradation process relates to adsorption/desorption processes on surface of NG films. Despite that aging effect, E-gun FE current demonstrated good stability on minute timescale with noise level not exceeding 3% (see inset of Fig. 3). Inevitable lowering of the current level observed during long-term operation may be compensated by corresponding increase of the voltage generated by control electronics. The test results demonstrated that the E-gun with NG cathode satisfy requirements for usage in the E-sail estimated in previous works [2,9].

The FE patterns of used NG cathodes were analyzed again in the same laboratory conditions after the E-gun tests. Images in Fig. 4a–c show the FE patterns of three NG cathodes with different degree of degradation of their emissivity occurred because of the E-gun testing at different regimes. After the tests FE pattern demonstrated strongly inhomogeneous distribution of emission sites correspondingly to the anode-mesh configuration. The emission disappeared completely in the border areas of the cathode where NG film was in touch with the kapton spacer. This was because of

irreversible changes in the morphology of the film as a result of mechanical compression of the flexible FLG flakes. Density of emission sites remains to be close to that in as-grown NG films in the peripheral areas, located under the cooper coated Si-Si₃N₄-Cu frame of the mesh anode during E-gun test measurements. In the central area of the tested cathodes density of emission sites is much smaller in comparison with that for the peripheral area and corresponds to the mesh configuration (Fig. 4a).

Depending on test duration and integral emission current, the samples demonstrate different densities of emission sites in the central area of the cathodes. The dark spots, containing just few emission sites, on Fig. 4b correspond to six holes in the Si-Si₃N₄ frame, which supports the anode grid as shown on the Fig. 1. At the highest degree of degradation, whole central area of the cathode is dark (Fig. 4c), i.e. contains no emission sites. Inspection of this sample with optical microscope (Fig. 4d) shows that a part of the graphitic material was completely removed from the cathode surface in the areas corresponding to the holes in the anode Si-Si₃N₄ frame. It may be explained by significant local increase of electric field strength (and corresponding emission current density) in the areas where electrostatic attraction produces reduction of anode-to-cathode distance because of flexibility of the mesh. The highest reduction of the anode-to-cathode distance and the most intensive cathode material destruction (due to Joule heating, ion bombardment, arcing, and Coulomb force acting between anode and cathode) occurs in the areas corresponding to the holes in the frame. These results indicate also that further improvement of the long-term characteristics of the E-gun is possible by creating an anode mesh with better mechanical stability preventing inhomogeneous decrease of the anode-to-cathode distance. The final E-gun launched with EstCube-1 was made using an anode with an electroformed nickel mesh bonded to a laser-cut nickel frame.

To reveal the structural changes and possible mechanism responsible for the degradation of the FE properties, the morphology of NG cathodes was examined with scanning electron microscopy (SEM). While this analysis has been performed for all samples, we will discuss further only results obtained for minimal level of FE degradation, corresponding to image (a) in Fig. 4. The SEM images made in backscattered electron (BSE) detection mode (Fig. 4e) shown no observable differences in NG film morphology before and after the E-gun tests and between central and peripheral areas of the tested cathode with low and high density of emission sites. However, on the SEM image made in secondary electron (SE) mode for the same boundary area of the cathode, passed through the E-gun test (Fig. 4f), the zone with reduced number of FE sites appeared much brighter than the peripheral area. The zoomed SEM images obtained with higher magnification revealed no observable differences in the structure and morphology of the NG crystallites in the both zones. A possible reason for this difference in the brightness of SEM image could be redeposition of the anode material (copper) on the surface of NG flakes sputtered during E-gun operation. However, performed energy-dispersive X-ray (EDX) analysis has not detected presence of copper or other non-carbon impurities in whole NG film surface. This corresponds also to absence of any differences in SEM image obtained in BSE

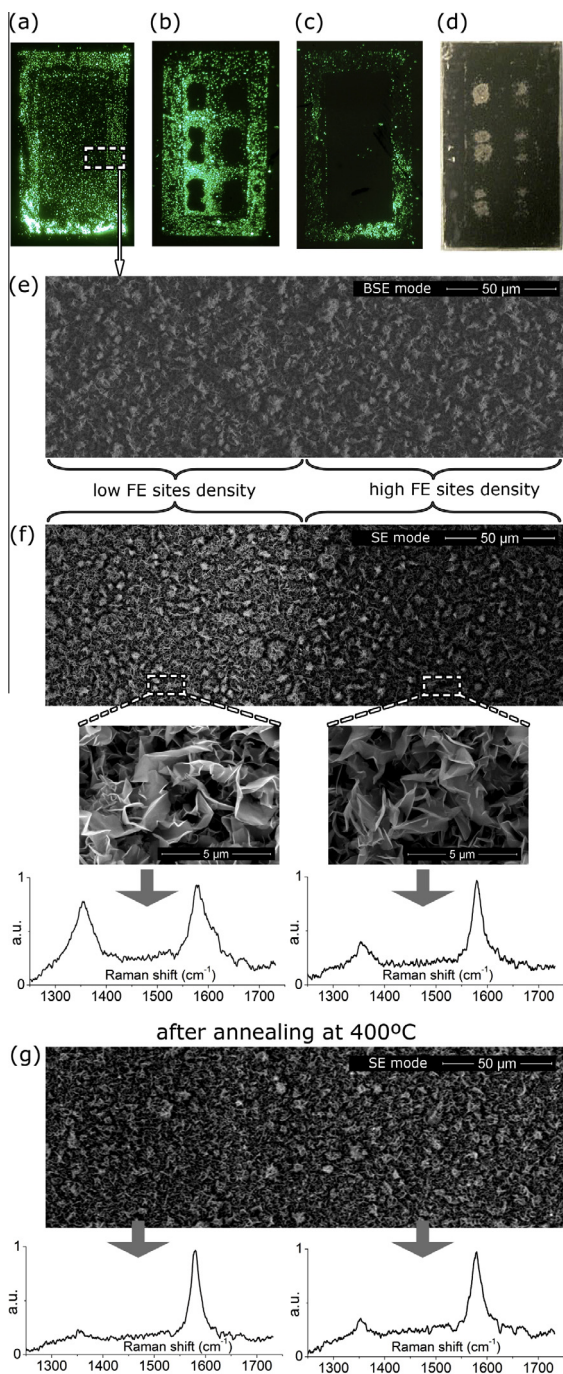


Fig. 4 – (a)–(c) FE patterns of NG cathodes after tests within E-gun assembly with different degree of FE degradation. (d) Optical photograph of the NG cathode, corresponding to the FE pattern (c). (e) SEM image of the NG cathode, made in back-scattering mode, for rectangular area marked in (a) and including zones with high and low density of emission sites. (f) SEM image of the same area, made in secondary electron detection mode; the zoom images made with higher magnification, and corresponding Raman spectra are shown below. (g) SEM image, made in secondary electron detection mode and corresponding Raman spectra of the same area after annealing at 400 °C. (A color version of this figure can be viewed online.)

mode (Fig. 4e) which is sensitive to surface contamination species with higher atomic number Z because of strong dependence of probability of electron elastic scattering on Z [11].

Raman spectroscopy of the NG cathodes revealed that the characteristic graphite peaks G at about 1580 cm^{-1} and D at about 1350 cm^{-1} are much broader in the FE degraded zone as shown on Fig. 4f. The broadening of the Raman peaks may indicate that the surface of the NG cathode is covered by amorphous carbon, produced during the E-gun tests, because of sputtering of cathode material by ion bombardment process [12]. Thus, the observed change in the brightness of the SEM image in SE mode also could be explained by presence of amorphous carbon material, which may affect the probability of secondary electron emission (and brightness of SEM image, correspondingly) [13].

In order to eliminate the amorphous carbon phase, the NG cathodes were thermally oxidized by exposing to heating in air at temperature of 400 °C for 30 min. As a result of this treatment, the difference in brightness of the SEM image disappeared completely and Raman spectrum in the FE degraded zone recovered to that corresponding to as-grown material (Fig. 4g). However, the FE properties had not changed after this thermal oxidation, meaning that the presence of the amorphous carbon on the surface of NG cathode does not influence significantly on its emission ability. We suppose that the degradation of FE properties during E-gun tests may be explained by removal of the most efficient FE centers having the lowest work function and the highest aspect ratio. These centers originate in as-grown material from sp^3 clusters located on the edges of the NG flakes [7,8]. Similar sp^3 clusters may appear on surface of the needle-like carbon nanostructures with twisted polygonal morphology presented in some amount in the NG film material [8,14]. Destruction of these sp^3 clusters is the most probable during the E-gun test, because they are located in the utmost tiny parts of the NG material.

4. Conclusion

Nanographite films produced by carbon condensation with use plasma enhanced chemical vapor deposition techniques were analyzed as highly efficient electron source (field emission cold cathode). The test measurements were performed within E-gun assembly designed for use in E-sail space thruster. It was shown that the FE current of the NG cold cathodes gradually decreases with time during long-term measurements at constant applied voltage in two stages with characteristic times of about 20 and 500–1000 h. It was revealed that after the tests the NG cathode surface was covered with amorphous carbon produced by sputtering of the graphitic material by ion bombardment. Elimination of the amorphous carbon had not led to the recovery of the FE properties. We believe that the FE degradation is determined by destruction of the most efficient FE sites having the lowest effective work function and the highest aspect ratios. While obtained characteristics of the NG cathodes fully satisfy the requirements of the E-gun on efficiency and stability, and could be used in

E-sail space thruster, further improvement of the E-gun is possible via more appropriate design of the anode electrode. The test mission satellite ETSCube-1 with a refined NG cathode E-gun onboard was launched in 2013, and now the first results on the electrical sail effect in low Earth orbit are expected.

Acknowledgments

This work was partially supported by the FP7 Marie Curie Program (Grant PIRSES-GA-2011-295241). VIK, EAS, ASO, and ANO are also grateful for financial support from Russian Science Foundation (Grant #14-12-00511).

REFERENCES

- [1] Janhunen P. Electric sail for spacecraft propulsion. *J Propul Power* 2004;20:763–4.
- [2] Janhunen P, Toivanen PK, Polkko J, Merikallio S, Salminen P, Haeggström E, et al. Electric solar wind sail: toward test missions. *Rev Sci Instrum* 2010;81:111301.
- [3] Gomer R. Field emission and field ionization. New York: AIP; 1993.
- [4] Xua NS, Ejaz Huq S. Novel cold cathode materials and applications. *Mater Sci Eng R* 2005;48:47–189.
- [5] Pajusalu M, Rantsus R, Pelakauskas M, Leitu A, Kalde J, Ilbis E, et al. Design of the electrical power system for the ESTCube-1 satellite. *Latvian J Phys Tech Sci* 2012;49:16–24.
- [6] Obraztsov AN, Zolotukhin AA, Ustinov AO, Volkov AP, Svirko Y, Jefimovs K. In situ plasma diagnostics for chemical vapor deposition of nano-carbon thin film materials. *Microelectron Eng* 2003;69:446–51.
- [7] Obraztsov AN, Kleshch VI. Cold and laser stimulated electron emission from nanocarbons. *J Nanoelectron Optoelectron* 2009;4:207–19.
- [8] Obraztsov AN, Kleshch VI, Smolnikova EA. A nano-graphite cold cathode for an energy-efficient cathodoluminescent light source. *Beilstein J Nanotechnol* 2013;4:493–500.
- [9] Janhunen P, Quarta AA, Mengali G. Electric solar wind sail mass budget model. *Geosci Instrum Method Data Syst* 2013;2:85–95.
- [10] Vasilieva EA, Kleshch VI, Obraztsov AN. Effect of residual gas pressure on field electron emission from nanographite films. *J Nanoelectron Optoelectron* 2012;7:41–5.
- [11] Goldstein J, Newbury D, Echlin P, Joy D, Lyman Ch, Lifshin E, et al. Scanning electron microscopy and X-ray microanalysis. New York: Kluwer Academic/Plenum Publishers; 2003.
- [12] Chu PK, Li L. Characterization of amorphous and nanocrystalline carbon films. *Mater Chem Phys* 2006;96:253–77.
- [13] Lang B. Carbon surfaces: relation between secondary electron spectrum and long-range order. *Surf Sci* 1979;80:38–44.
- [14] Chuvilin AL, Kuznetsov VL, Obraztsov AN. Chiral carbon nanoscrolls with a polygonal cross-section. *Carbon* 2009;47:3099–105.